EWASG: A Equation-of-State Module for Water, NaCl, Non-Condensible Gas

Yoojin Jung
George Pau
Stefan Finsterle

Earth Sciences Division, Lawrence Berkeley National Laboratory
University of California, Berkeley, California 94720

1. Description

1.1. Thermophysical Properties

The EWASG (**WA**ter-**S**alt-**G**as) fluid property module was developed by Battistelli et al. (1997) for modeling geothermal reservoirs with saline fluids and non-condensible gas (NCG). In contrast to EOS7, EWASG describes aqueous fluid of variable salinity not as a mixture of water and brine, but as a mixture of water and NaCl. This makes it possible to represent temperature-dependent solubility constraints, and to properly describe precipitation and dissolution of salt. EWASG represents the active system components (water, NaCl, NCG) as three-phase mixtures. Solid salt is the only active mineral phase, and is treated in complete analogy to fluid phases (aqueous, gas), except that, being immobile, its relative permeability is identically zero. From mass balances on salt in fluid and solid phases we calculate the volume fraction of precipitated salt in the original pore space ϕ_0, which is termed "solid saturation," and denoted by S_S. A fraction $\phi_0 S_S$ of reservoir volume is occupied by precipitate, while the remaining void space $\phi_f = \phi_0 (1 - S_s)$ is available for fluid phases. We refer to ϕ_f as the "active flow porosity." The reduction in pore space reduces the permeability of the medium (see Section 1.2).

Several choices are available for the non-condensible gas (NCG): CO_2, air, CH_4, H_2, and N_2. Gas dissolution in the aqueous phase is described by Henry's law, with coefficients that depend not only on temperature but also on salinity to describe the reduction in NCG solubility with increasing salinity ("salting out"). The dependence of brine density, enthalpy, viscosity, and vapor pressure on salinity is taken into account, as are vapor pressure-lowering effects from suction pressures (capillary and vapor adsorption effects). The thermophysical property correlations used in EWASG are accurate for most conditions of interest in geothermal reservoir studies: temperatures in the range from 100 to 350 ˚C, fluid pressures up to 80 MPa, CO_2 partial pressures up to 10 MPa, and salt mass fraction up to halite saturation. With the exception of brine enthalpy, thermophysical property correlations are accurate to below 10 ˚C. A full discussion of the thermophysical property correlations used and their empirical basis is given in the original paper (Battistelli et al., 1997).

TOUGH3 also adopts recent improvements of EWASG. Internally consistent correlations for the water-NaCl mixture properties are included (Battistelli, 2012), which are developed by Driesner and Heinrich (2007) and Driesner (2007). These brine correlations are capable to calculate phase properties for temperatures from 0 to 350 ˚C, pressures from 1 to 100 MPa, and

salt mass fraction up to saturation. In TOUGH3, the brine correlations in Driesner (2007) are used as the default, unless specified differently by users.

New options are also added to calculate NCG (CO_2, CH_4, and H_2 only) density and fugacity using a virial equation treatment of Spycher and Reed (1988). This method is available and reliable only for the following temperature and pressure ranges: 1) for CO_2, 50 – 350 ˚C and up to 50 MPa, 2) for CH_4, 16 – 350 ˚C and up to 50 MPa, and 3) for H_2, 25 – 600 ˚C and up to 300 MPa.

1.2. Permeability Change

As noted above, the relationship between the amount of solid precipitation and the pore space available to the fluid phases is very simple. The impact of porosity change on formation permeability on the other hand is highly complex. Laboratory experiments have shown that modest reductions in porosity from chemical precipitation can cause large reductions in permeability (Vaughan, 1987). This is explained by the convergent-divergent nature of natural pore channels, where pore throats can become clogged by precipitation while disconnected void spaces remain in the pore bodies (Verma and Pruess, 1988). The permeability reduction effects depend not only on the overall reduction of porosity but on details of the pore space geometry and the distribution of precipitate within the pore space. These may be quite different for different porous media, which makes it difficult to achieve generally applicable, reliable predictions. EWASG offers several choices for the functional dependence of relative change in permeability, k/k_0, on relative change in active flow porosity.

$$\frac{k}{k_0} = f\left(\frac{\phi_f}{\phi_0}\right) \equiv f\left(1 - S_s\right) \tag{1}$$

The simplest model that can capture the converging-diverging nature of natural pore channels consists of alternating segments of capillary tubes with larger and smaller radii, respectively; see Figure 1. While in straight capillary tube models permeability remains finite as long as porosity is non-zero, in models of tubes with different radii in series, permeability is reduced to zero at a finite porosity.

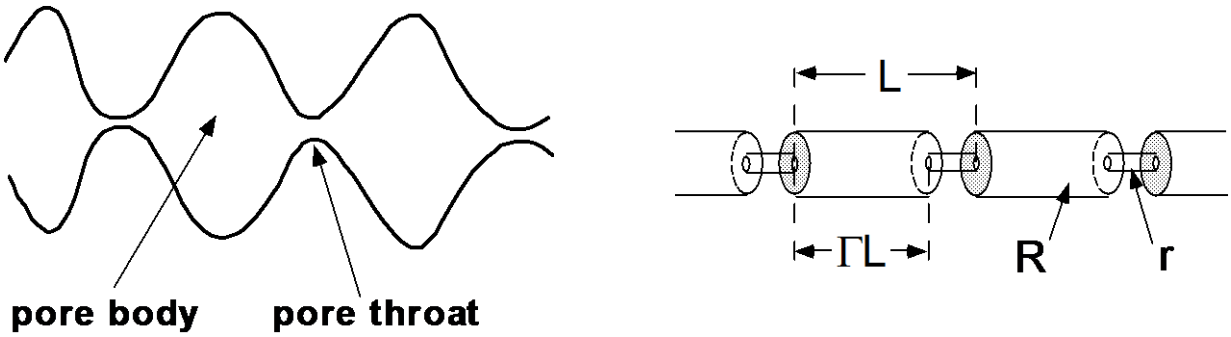

(a) conceptual model (b) tubes-in-series

Figure 1. Model for converging-diverging pore channels.

From the tubes-in-series model shown in Figure 1, the following relationship can be derived (Verma and Pruess, 1988)

$$\frac{k}{k_0}=\theta^2\frac{1-\Gamma+\Gamma/\omega^2}{1-\Gamma+\Gamma\left[\theta/\left(\theta+\omega-1\right)\right]^2} \tag{2}$$

Here

$$\theta=\frac{1-S_s-\phi_r}{1-\phi_r} \tag{3}$$

depends on the fraction 1-S_s of original pore space that remains available to fluids, and on a parameter ϕ_r, which denotes the fraction of original porosity at which permeability is reduced to zero. Γ is the fractional length of the pore bodies, and the parameter ω is given by

$$\omega=1+\frac{1/\Gamma}{1/\phi_r-1} \tag{4}$$

Therefore, Eq. (2) has only two independent geometric parameters that need to be specified, ϕ_r and Γ. As an example, Figure 2 shows the permeability reduction factor from Eq. (2), plotted against $\phi/\phi_0\equiv\left(1-S_s\right)$, for parameters of ϕ_r = Γ = 0.8.

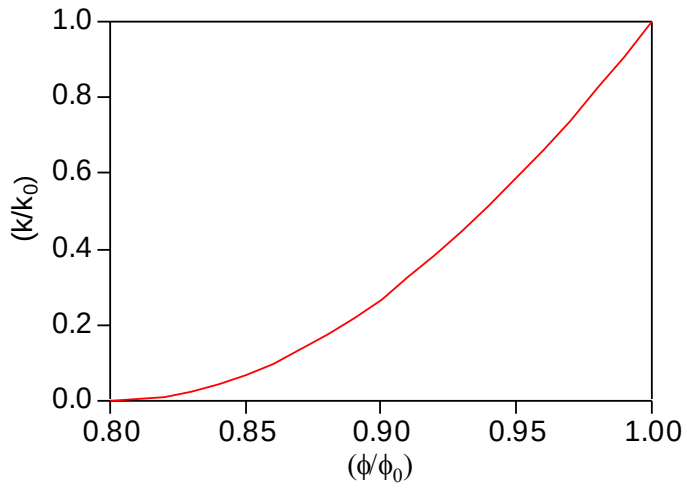

Figure 2. Porosity-permeability relationship for tubes-in-series model, after Verma and Pruess (1988).

For parallel-plate fracture segments of different aperture in series, a relationship similar to Eq. (2) is obtained, the only difference being that the exponent 2 is replaced everywhere by 3 (Verma and Pruess, 1988). If only straight capillary tubes of uniform radius are considered, we have $\phi_r = 0$, $\Gamma = 0$, and Eq. (2) simplifies to

$$k/k_0 = (1 - S_s)^2 \tag{5}$$

2. Specifications

A summary of EWASG specifications and parameters appears in **Error! Reference source not found.**. The default parameter settings are (*NK*, *NEQ*, *NPH*, *NB*) = (3, 4, 3, 6). The *NK* = 2 (no air) option may only be used for problems with single-phase liquid conditions throughout. The primary variables are (P, X_{sm}, X_3, T) for single-phase conditions and (P, X_{sm}, S_g+10, T) for two-phase conditions.

Primary variable # 2 ($X2$) is used for NaCl, and denotes mass fraction X_s in the aqueous phase when no solid salt is present, while it is solid saturation plus ten (S_s + 10) in the presence of precipitated salt. The number 10 is added here to be able to determine whether or not a precipitated phase is present from the numerical range of the second primary variable. Solubility

of NaCl in the gas phase is very small at the pressure and temperature conditions considered for EWASG and has been neglected. During the Newton-Raphson iteration process, possible appearance or disappearance of a solid phase is checked, as follows. If no solid phase was present at the previous iteration, primary variable *X2* is known to denote salt mass fraction X_s in the aqueous phase, and the latest updated value is compared with the equilibrium solubility *XEQ*. If $S_s > XEQ$, precipitation starts, a small solid phase saturation is initialized as $S_s = 10^{-6}$, and the second primary variable is switched to $X2 = S_s + 10$. If solid salt had been present at the previous iteration, EWASG checks whether $S_s = X2 - 10$ is still larger than 0. If not, this indicates that the solid phase disappears; the second primary variable is then switched to dissolved salt mass fraction, and is initialized just below equilibrium solubility as $S_s = XEQ - 10^{-6}$.

Table 1. Summary of EWASG

<u>Components</u>	# 1: water # 2: NaCl # 3: NCG (CO_2, air, CH_4, H_2, N_2; optional)
<u>Parameter choices</u> (*NK*, *NEQ*, *NPH*, *NB*) =	(3, 4, 3, 6) water, NaCl, NCG, nonisothermal (default) (3, 3, 3, 6) water, NaCl, NCG, isothermal (2, 3, 2, 6) water, NaCl, nonisothermal† (2, 2, 2, 6) water, NaCl, isothermal†
molecular diffusion can be modeled by setting *NB* = 8	
<u>Primary Variables</u> single fluid phase (only liquid, or only gas) (P, X_{sm}, X_3, T) - (pressure, salt mass fraction X_s or solid saturation S_s+10, NCG mass fraction, temperature) two fluid phases (liquid and gas)& (P, X_{sm}, S_g+10, T) - (pressure, salt mass fraction X_s or solid saturation S_s+10, gas phase saturation S_g+10, temperature)	

† the *NK* = 2 (no NCG) option may only be used for problems with single-phase liquid conditions throughout

& two-phase conditions may be initialized with variables (T, X_{sm}, S_g+10, P_{NCG}), or (T, X_{sm}, S_g+10, X_3), where P_{NCG} is the partial pressure of *NCG*, X_3 is mass fraction of *NCG* in the liquid phase; by convention, EWASG will assume the first primary variable to be pressure if it is larger than 370, otherwise it will be taken to be temperature; if the first primary variable is temperature, the last primary variable will be

taken to mean mass fraction of *NCG* if it is less than 1, otherwise it will be taken to mean *NCG* partial pressure

Various options for EWASG can be selected through parameter specifications in data block **SELEC**, as follows.

SELEC keyword to introduce a data block with parameters for EWASG.

Record **SELEC**.1

Format (16I5)
IE(I), I=1,16

IE(1) set equal to 1, to read one additional data record (a larger value with more data records is acceptable, but only one additional record will be used by EWASG).

IE(3) allows choice of brine viscosity calculation.

0: after Phillips et al. (1981) (default).

1: after Palliser and McKibbin (1998).

2: after Mao and Sun (2006).

3: after Potter (1978).

IE(4) allows choice of correlation for compressed brine density.

1: after Andersen et al. (1992) (default = 0).

2: Pritchett (1993).

3: Brine compressibility equal to water compressibility at the same reduced temperature.

4: Brine compressibility equal to water compressibility at the same temperature.

5: after Batzle and Wang (1992).

6: after Driesner (2007) .

IE(8) allows choice of NCG density and fugacity calculation.

0: original EWASG approach (default).

1: NCG density according to Spycher and Reed (1988). Only for CO_2, CH_4, and H_2.

2: NCG density and gas-aqueous equilibrium according to Spycher and Reed (1988). Only for CO_2, CH_4, and H_2.

IE(9) allows choice of NCG enthalpy calculation in the aqueous phase.

0: original EWASG approach (default).

1: NCG enthalpy as a function of temperature.

IE(10) allows to turn vapor pressure lowering on/off.

0: VPL is off.

1: VPL is on.

IE(11) selects dependence of permeability on the fraction $\phi_f / \phi_0 = (1 - S_s)$ of original pore space that remains available to fluids.

0: permeability does not vary with ϕ_f.

1: $k/k_0 = (1 - S_s)^{\gamma}$, with γ = *FE(1)* (record **SELEC**.2).

2: fractures in series, i.e., Eq. (2) with exponent 2 everywhere replaced by 3.

3: tubes-in-series, i.e., Eq. (2).

IE(14) allows choice of treatment of thermophysical properties as a function of salinity

0: full dependence (default).

1: vapor pressure independent of salinity.

2: vapor pressure and brine enthalpy independent of salinity.

3: no salinity dependence of thermophysical properties (salt solubility constraints are maintained).

IE(15) allows choice of correlation for brine enthalpy at saturated vapor pressure

1: after Michaelides (1981).

2: after Miller (1978). (obsolete)

3: after Phillips et al. (1981).

4: after Lorenz et al. (2000) (default = 0).

5: after Driesner (2007).

IE(16) allows choice of the type of NCG (default for *IE(16)*=0 is CO_2)

1: air

2: CO_2

3: CH_4

4: H_2

5: N_2

Record **SELEC**.2 introduces parameters for functional dependence of permeability on solid saturation

Format (8E10.4)
FE(1), FE(2)

FE(1) parameter γ (for *IE(11)*=1); parameter ϕ_r (for *IE(11)* = 2, 3)

FE(2) parameter Γ (for *IE(11)* = 2, 3)

3. Sample Problems

3.1. Problem No. 1 (*dnh*) - Brine Density Calculation

This problem demonstrates the newly implemented brine correlations. Figure 3 shows the input file. Several element subproblems are simulated, which are entirely independent of each other (no flow connections between subproblems), except that being run together they all must go through the same sequence of time steps. Only a single time step (1E-8 sec) is computed to calculate the brine density at different initial salt mass fraction. The salt content approximately varies from 1 to 6 molal. *IE(4)* = 6 is specified in data block **SELEC** to compute the brine density according to Driesner (2007). Data block **OUTPU** is used to select the liquid density as a single print-out variable. Figure 4 shows the result using the input file shown in Figure 3, and Figure 5 shows the result using the option *IE(4)* = 1 and *IE(15)* = 4 (note that if only either the brine density (*IE(4)*) or enthalpy (*IE(15)*) is specified to use the Driesner's correlation, TOUGH3 internally assigns the other brine property uses the Driesner's correlation as well). The brine densities are slightly overestimated with *IE(4)* = 1, compared to those by Driesner (2007). A more comprehensive comparison between different approaches is shown in Battistelli (2012).

```
*dnh* CODE DEMONSTRATION: BRINE DENSITY CALCULATION
ROCKS----1----*----2----*----3----*----4----*----5----*----6----*----7----*----8
TRANS          2650.       .50    1.E-14                          2.10     1000.

START----1----*----2----*----3----*----4----*----5----*----6----*----7----*----8
----*----1 MOP: 123456789*123456789*1234 ---*----5----*----6----*----7----*----8
PARAM----1----*----2----*----3----*----4----*----5----*----6----*----7----*----8
   2   1       1100 30 000000000711
                         -1.
     1.E-8

              800.E5              0.E-03                 0.0                300.

RPCAP----1----*----2----*----3----*----4----*----5----*----6----*----7----*----8
    3            .30       .05
    1                       1.
ELEME----1----*----2----*----3----*----4----*----5----*----6----*----7----*----8
F   1    5    1TRANS        1.

CONNE----1----*----2----*----3----*----4----*----5----*----6----*----7----*----8


SELEC----1----*----2----*----3----*----4----*----5----*----6----*----7----*----8
    1              6

OUTPU----1----*----2----*----3----*----4----*----5----*----6----*----7----*----8
    1
DENSITY                2
```

Figure 3. Input file for brine density calculation.

```
INCON ---1----*----2----*----3----*----4----*----5----*----6----*----7----*----8
F   1
              800.E5              50.E-03                 0.0                 300.
F   2
              800.E5             100.E-03                 0.0                 300.
F   3
              800.E5             150.E-03                 0.0                 300.
F   4
              800.E5             200.E-03                 0.0                 300.
F   5
              800.E5             250.E-03                 0.0                 300.
F   6
              800.E5             300.E-03                 0.0                 300.

ENDCY----1----*----2----*----3----*----4----*----5----*----6----*----7----*----8
```

Figure 3. Input file for brine density calculation (continued).

```
"              ELEM","             DEN_L"
"                  ","          (KG/M**3)"
"TIME [sec]  0.10000000E-07"
"              F   1",  0.85026618087E+003
"              F   2",  0.89251882680E+003
"              F   3",  0.93441086845E+003
"              F   4",  0.97667542936E+003
"              F   5",  0.10198049242E+004
"              F   6",  0.10641579666E+004
```

Figure 4. Brine densities in CSV format based on **OUTPU** block shown in Figure 3 (*IE(4)* = 6).

```
"              ELEM","             DEN_L"
"                  ","          (KG/M**3)"
"TIME [sec]  0.10000000E-07"
"              F   1",  0.86241240961E+003
"              F   2",  0.89902058934E+003
"              F   3",  0.94534726201E+003
"              F   4",  0.99802610553E+003
"              F   5",  0.10571463068E+004
"              F   6",  0.11286262099E+004
```

Figure 5. Brine densities in CSV format when *IE(4)* = 1 and *IE(15)* = 4 is used.

3.2. Problem No. 2 (*rhbc*) - Production from a Geothermal Reservoir with Hypersaline Brine and CO_2

This problem examines production from a hypothetical geothermal reservoir with high salinity and CO_2. A single well produces at a constant rate of 65 kg/s from an infinite-acting reservoir in 1-D radial flow geometry. The reservoir is in two-phase conditions initially, with uniform initial conditions of P = 60 bar, T = 275.55 ˚C; other problem parameters are given in Table 2, and Figure 6 shows the TOUGH3 input file. The choices made with **SELEC**-data are: no vapor pressure lowering (*IE(10)* = 0), a tubes-in-series model for permeability reduction from precipitation (*IE(11)* = 3), full dependence of thermophysical properties on salinity (*IE(14)* = 0), Michaelides correlation for brine enthalpy (*IE(15)* = 1), and CO_2 as non-condensible gas (*IE(16)* = 2). The permeability-porosity relationship for the parameters used here (*IE(11)* = 3, *FE(1)* = *FE(2)* = 0.8) is shown in Figure 6.

Table 2. Parameters for production from a saline reservoir with CO_2.

Reservoir thickness	500 m
Permeability	50×10^{-15} m^2
Porosity	0.05
Relative permeability Corey curves with S_{lr} = S_{gr} =	 0.30 0.05
Rock grain density	2600 kg/m^3
Specific heat	1000 J/kg ˚C
Thermal conductivity	2.1 W/m ˚C
Initial conditions	
Temperature	275.55 ˚C
Gas saturation	0.45
Pressure	60.0 bar
NaCl mass fraction in liquid phase	0.30
CO_2 partial pressure	14.79 bar
Wellblock radius	5 m
Production rate	65 kg/s

```
*rhbc*  - 1-D radial flow problem for EWASG, with NaCl and CO2
MESHMAKER1----*----2----*----3----*----4----*----5----*----6----*----7----*----8
RZ2D
RADII
    1
        5.
EQUID
    1             2.
LOGAR
   50           1.E2
LOGAR
   20           1.E3
EQUID
    1            0.0
LAYER----1----*----2----*----3----*----4----*----5----*----6----*----7----*----8
    1
      500.

ROCKS----1----*----2----*----3----*----4----*----5----*----6----*----7----*----8
POMED    2     2600.       .05   50.e-15   50.e-15   50.e-15       2.0    1000.0

    3     .30       .05
    1               1.

SELEC----2----3----4----5----6----7----8----9---10---11---12---13---14---15---16
    1                                          0    3    0    0    0    1    2
        .8   .8
     ..... IE(16) = 2 chooses CO2 .....
MULTI----1----*----2----*----3----*----4----*----5----*----6----*----7----*----8
    3    4    3    6
START----1----*----2----*----3----*----4----*----5----*----6----*----7----*----8
----*----1--MOP:123456789012345678901234----*----5----*----6----*----7----*----8
PARAM----1----*----2----*----3----*----4----*----5----*----6----*----7----*----8
   1 100     100100 0000000000 40 0 3
               2.e6       -1.
      1.E4
     1.E-5     1.E00                                  1.E-7
               60.e5                 .30              10.45              275.55
TIMES----1----*----2----*----3----*----4----*----5----*----6----*----7----*----8
    1    1
      5.e5
RPCAP----1----*----2----*----3----*----4----*----5----*----6----*----7----*----8
    3     .30       .05
    1               1.
INCON----1----*----2----*----3----*----4----*----5----*----6----*----7----*----8

GENER----1----*----2----*----3----*----4----*----5----*----6----*----7----*----8
A1  1wel 1                        MASS       -65.

ENDCY----1----*----2----*----3----*----4----*----5----*----6----*----7----*----8
```

Figure 6. TOUGH3 input file for constant-rate production from 1-D cylindrical reservoir.

Fluid withdrawal causes pressures to drop near the production well. Boiling of reservoir fluid gives rise to dilution of CO_2 in the gas phase and to increased concentrations of dissolved NaCl, which begins to precipitate when the aqueous solubility limit is reached. As the boiling front recedes from the well, solid precipitate fills approximately 10 % of the original void space (see Figure 7), causing permeability to decline to approximately 28 % of its original value.

Specifications of this problem (1-D radial geometry, uniform initial conditions, constant well rate) were chosen so that a similarity solution would be applicable, which should depend on radius R and time t only through the similarity variable $x = R^2/t$ (O'Sullivan, 1981). This similarity property should hold even when all complexities of two-phase flow with nonlinear relative permeabilities, CO_2 exsolution effects, salt precipitation, and associated porosity and permeability effects are taken into account. The agreement between results for two different times (5×10^5 and 2×10^6 seconds) when plotted as a function of the similarity variable shows that the similarity property holds very accurately for all thermodynamic variables (Figure 7). As a benchmark for proper code installation, we also provide printout for the first few time steps of the TOUGH3 run, Figure 8.

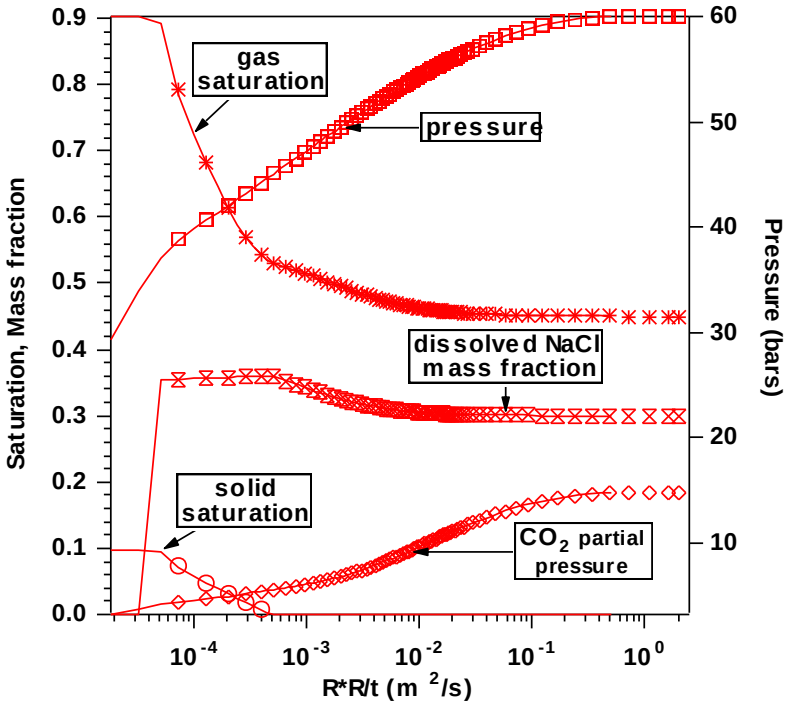

Figure 7. Simulated thermodynamic conditions for 1-D radial flow problem with salinity and non-condensible gas, plotted as a function of the similarity variable $x = R^2/t$. Results at 2×10^6 seconds are shown as lines, while the data at $t = 5 \times 10^5$ seconds are given as symbols.

```
...ITERATING... AT [    1, 1] --- DELTEX = 0.100000E+05  MAX. RES. = 0.588732E+01 AT ELEMENT A1  1  EQUATION   3
...ITERATING... AT [    1, 2] --- DELTEX = 0.100000E+05  MAX. RES. = 0.174152E+01 AT ELEMENT A1  1  EQUATION   3
...ITERATING... AT [    1, 3] --- DELTEX = 0.100000E+05  MAX. RES. = 0.149414E+00 AT ELEMENT A1  1  EQUATION   3
...ITERATING... AT [    1, 4] --- DELTEX = 0.100000E+05  MAX. RES. = 0.140834E-02 AT ELEMENT A1  1  EQUATION   3
A1  1(    1, 5) ST = 0.100000E+05 DT = 0.100000E+05
...ITERATING... AT [    2, 1] --- DELTEX = 0.100000E+05  MAX. RES. = 0.154657E+00 AT ELEMENT A1  1  EQUATION   3
...ITERATING... AT [    2, 2] --- DELTEX = 0.100000E+05  MAX. RES. = 0.120701E-01 AT ELEMENT A1  1  EQUATION   3
A1  1(    2, 3) ST = 0.200000E+05 DT = 0.100000E+05
...ITERATING... AT [    3, 1] --- DELTEX = 0.200000E+05  MAX. RES. = 0.918525E-01 AT ELEMENT A1  1  EQUATION   1
...ITERATING... AT [    3, 2] --- DELTEX = 0.200000E+05  MAX. RES. = 0.407405E-01 AT ELEMENT A1  1  EQUATION   3
...ITERATING... AT [    3, 3] --- DELTEX = 0.200000E+05  MAX. RES. = 0.809826E-04 AT ELEMENT A1  1  EQUATION   3
A1  1(    3, 4) ST = 0.400000E+05 DT = 0.200000E+05
...ITERATING... AT [    4, 1] --- DELTEX = 0.400000E+05  MAX. RES. = 0.102536E+00 AT ELEMENT A1  1  EQUATION   1
...ITERATING... AT [    4, 2] --- DELTEX = 0.400000E+05  MAX. RES. = 0.816845E+00 AT ELEMENT A1  1  EQUATION   3
...ITERATING... AT [    4, 3] --- DELTEX = 0.400000E+05  MAX. RES. = 0.655684E-02 AT ELEMENT A1  1  EQUATION   3
A1  1(    4, 4) ST = 0.800000E+05 DT = 0.400000E+05
...ITERATING... AT [    5, 1] --- DELTEX = 0.800000E+05  MAX. RES. = 0.143439E+00 AT ELEMENT A1  1  EQUATION   1
...ITERATING... AT [    5, 2] --- DELTEX = 0.800000E+05  MAX. RES. = 0.190164E+01 AT ELEMENT A1  2  EQUATION   3
...ITERATING... AT [    5, 3] --- DELTEX = 0.800000E+05  MAX. RES. = 0.625453E-01 AT ELEMENT A1  2  EQUATION   3
...ITERATING... AT [    5, 4] --- DELTEX = 0.800000E+05  MAX. RES. = 0.196693E-04 AT ELEMENT A1  2  EQUATION   3
A1  1(    5, 5) ST = 0.160000E+06 DT = 0.800000E+05
```

Figure 8. Iteration sequence for first five time steps of the hypersaline reservoir problem.

References

Andersen, G., A. Probst, L. Murray, and S. Butler, An accurate PVT model for geothermal fluids as represented by H2O-CO2-NaCl mixtures. Proceedings, Seventeenth Workshop on Geothermal Reservoir Engineering, 17:239–248. Stanford University, Stanford, Calif., January 29-31, 1992.

Battistelli, A., C. Calore and K. Pruess. The Simulator TOUGH2/EWASG for Modeling Geothermal Reservoirs with Brines and Non-Condensible Gas, *Geothermics*, Vol. 26, No. 4, pp. 437 - 464, 1997.

Battistelli, A. Improving the Treatment of Saline Brines in EWASG for the Simulation of Hydrothermal Systems. In: Finsterle et al. (Eds.), Proceedings of the TOUGH Symposium 2012. Report LBNL-5808E. Lawrence Berkeley National Laboratory, Berkeley, Calif., 2012.

Batzle, M. and Wang, Z. 1992. Seismic properties of pore fluids. Geophysics 57 (11): 1396–1408.

Driesner T., and C.H. Heinrich. The system H2O–NaCl. Part I: Correlation formulae for phase relations in temperature–pressure–composition space from 0 to 1000°C, 0 to 5000 bar, and 0 to 1 XNaCl, *Geoch. Cosm. Acta*, 71, 4880–4901, 2007.

Driesner T., The system H2O–NaCl. Part II: Correlations for molar volume, enthalpy, and isobaric heat capacity from 0 to 1000°C, 1 to 5000 bar, and 0 to 1 XNaCl, *Geoc. Cosm. Acta*, 71, 4902–4919, 2007.

Lorenz S., D. Maric, and C. Rirschl, Eine analytische Funktion zur Bestimmung der Enthalpie wässriger NaCl-Lösungen. Rapporto ISTec - A – 447, 2000.

Mao S. and Z. Duan, The Viscosity of Aqueous Alkali-Chloride Solutions up to 623 K, 1,000 bar, and High Ionic Strength. *Int J Thermophys*, 30:1510–1523, 2006.

Michaelides, E.E. Thermodynamic Properties of Geothermal Fluids, Geothermal Resources Council Transactions, Vol. 5, pp. 361 - 364, 1981.

Miller, A.B. A Brine-Steam Properties Computer Program for Geothermal Energy Calculations, Lawrence Livermore National Laboratory Report UCRL-52495, Livermore, CA, June 1978.

O'Sullivan, M.J., A Similarity Method for Geothermal Well Test Analysis, *Water Resour. Res.*, Vol. 17, No. 2, pp. 390 – 398, 1981.

Palliser C., and R. McKibbin, A model for deep geothermal brines. I. T–P–X state–space description. *Transp. Por. Med.*, 33, 65–80, 1998.

Phillips, S. L., A. Igbene, J.A. Fair, H. Ozbek, and M. Tavana, A technical databook for geothermal energy utilization, Lawrence Berkeley Laboratory Report LBL-12810, Berkeley, Calif., 1981.

Potter R.W. II, Viscosity of Geothermal Brines. GRC Trans., Geothermal Resource Council, 2, 543-44, 1978.

Spycher N.F. and M.H. Reed, Fugacity coefficients of H_2, CO_2, CH_4, H_2O and H_2O-CO_2-CH_4 mixtures: A virial equation treatment for moderate pressures and temperatures applicable to hydrothermal boiling. *Geochim. Cosmochim. Acta* 52, 739–749, 1988.

Vaughan, P.J. Analysis of Permeability Reduction During Flow of Heated, Aqueous Fluid Through Westerly Granite, in C.F. Tsang (ed.), *Coupled Processes Associated with Nuclear Waste Repositories*, pp. 529 - 539, Academic Press, New York, 1987.

Verma, A. and K. Pruess, Thermohydrologic Conditions and Silica Redistribution Near High-Level Nuclear Wastes Emplaced in Saturated Geological Formations, *J. of Geophys. Res.*, Vol. 93, No. B2, pp. 1159-1173, 1988.